

## OUTER LAYERS OF A CARBON STAR: THE VIEW FROM THE *HUBBLE SPACE TELESCOPE*

HOLLIS R. JOHNSON<sup>1</sup> AND LISA M. ENSMAN

Indiana University, Astronomy Department, Swain West 319, Bloomington, IN 47405;  
 johnsonh@ucs.indiana.edu, lisa@kochab.astro.indiana.edu

DAVID R. ALEXANDER

Wichita State University, Physics Department, Wichita, KS 67208; dra@twsvvm.uc.twsu.edu

EUGENE H. AVRETT

Center for Astrophysics, Smithsonian Astrophysical Observatory, 60 Garden Street, Cambridge, MA 02138; avrett@cfasp22.harvard.edu

ALEXANDER BROWN

University of Colorado, JILA, Campus Box 440, Boulder, CO 80309; ab@jila.bitnet

KENNETH G. CARPENTER

NASA-Goddard Space Flight Center, Code 681, Greenbelt, MD 20771; hrscarpenter@tma1.gsfc.nasa.gov

KJELL ERIKSSON AND BENGT GUSTAFSSON

Uppsala Astronomical Observatory, Box 515, S-751 20 Uppsala, Sweden; kjell.eriksson@astro.uu.se, bengt.gustafsson@astro.uu.se

UFFE G. JØRGENSEN

Niels Bohr Institute, Blegdamsvej 17, DK-2100 Copenhagen, Denmark; uffegj@nbivax.nbi.dk

PHILIP D. JUDGE

High Altitude Observatory, NCAR, P.O. Box 3000, Boulder, CO 80307; judge@hao.ucar.edu

JEFFREY L. LINSKY<sup>2</sup>

JILA, University of Colorado, and NIST, Campus Box 440, University of Colorado, Boulder, CO 80309-0440

DONALD G. LUTTERMOSER<sup>3</sup>

Applied Research Corporation, 8201 Corporate Drive, Suite 1120, Landover, MD 20785; lutter@fosvax.arcch.com

FRANCOIS QUERCI AND MONIQUE QUERCI

Observatoire Midi-Pyrenees, 14 Avenue Edouard Belin, 31400 Toulouse, France; querci@obs-mip.fr

RICHARD D. ROBINSON

NASA-Goddard Space Flight Center, Code 681/CSC, Greenbelt, MD 20771; hrsrobinson@hrs.gsfc.nasa.gov

AND

ROBERT F. WING

Ohio State University, Astronomy Department, 174 West 18th Avenue, Columbus, OH 43210

Received 1994 August 19; accepted 1994 October 19

### ABSTRACT

To advance our understanding of the relationship between stellar chromospheres and mass loss, which is a common property of carbon stars and other asymptotic giant branch stars, we have obtained ultraviolet spectra of the nearby N-type carbon star UU Aur using the *Hubble Space Telescope* (*HST*). In this paper we describe the *HST* observations, identify spectral features in both absorption and emission, and attempt to infer the velocity field in the chromosphere, upper photosphere, and circumstellar envelope from spectral line shifts. A mechanism for producing fluoresced emission to explain a previously unobserved emission line is proposed. Some related ground-based observations are also described.

*Subject headings:* stars: carbon — stars: chromospheres — stars: mass loss — ultraviolet: stars

### 1. INTRODUCTION

Carbon stars are evolutionary advanced stars that lie high on the asymptotic giant branch (AGB), poised to become long-period variables (many already are) and then planetary nebulae. As significant contributors to heavy-element enrichment of the interstellar medium, they are important in under-

standing galactic evolution. Galactic enrichment of heavy elements (carbon and *s*-process elements) occurs as a by-product of the red-giant wind that eventually strips off the entire stellar envelope and exposes the future white dwarf inside. But the driving mechanisms for the wind are not well understood. In this paper we discuss recent observations of the N-type carbon star UU Aur = HR 2405 = HD 46678, particularly observations made with the *Hubble Space Telescope* (*HST*), which may provide clues to the processes that connect the mass flow to the photosphere and chromosphere.

The atmospheres of cool giants provide interesting regimes of temperature, density, and velocity. In particular, their chromospheres, which extend for a small fraction of a stellar

<sup>1</sup> Also Niels Bohr Institute, Blegdamsvej 17, 2100 Copenhagen, Denmark.

<sup>2</sup> Staff Member, Quantum Physics Division, National Institute of Standards and Technology.

<sup>3</sup> Visiting Astronomer, National Solar Observatory, operated by the Association of Universities for Research in Astronomy, Inc., under cooperative agreement with the National Science Foundation.

radius above the photosphere, are regions where considerable energy and momentum are imparted to the gas, generating winds but no high-temperature coronae. While the mechanism(s) for driving mass loss has not yet been completely specified, radiation pressure on grains provides an attractive possibility (cf. Knapp 1986; Sedlmayr 1994), although it may be aided or even replaced in some stars by pulsation-driven atmospheric extension (Bowen 1988; Bowen & Willson 1991), acoustic waves (Cuntz, Rammacher, & Ulmschneider 1994), or radiation pressure on molecules (Gustafsson & Plez 1992; Jørgensen & Johnson 1992). The chromospheres may also be inhomogeneous, that is, have only a fractional filling factor. Observational data from a variety of sources and wavelengths across the spectrum (Judge & Stencel 1991; Johnson 1991) suggest that one must search for the roots of mass loss in the photosphere-chromosphere region.

Despite recent advances (e.g., Rammacher & Cuntz 1991), our present limited knowledge of mechanisms for energy and momentum generation, transport, and deposition does not allow us to calculate realistic, self-consistent chromospheric or wind models from first principles. Instead, workers have adopted semiempirical methods to derive models which set constraints on the underlying mechanisms responsible for the observed structures. That is, different chromospheric temperature structures are superposed on a photospheric model, and that chromosphere model whose synthetic spectrum best matches the observations is chosen to represent the stellar chromosphere. Only one semiempirical, non-LTE (NLTE) chromospheric model for a carbon star (TX Psc) is available (Luttermoser et al. 1989, hereafter LJAL). In that one-dimensional model, a sharp temperature rise to 4000–6000 K was required to reproduce the observed emission. A similar chromospheric model for an M6 giant is also now available (Luttermoser, Johnson, & Eaton 1994). As noted by the authors, both of these models suffer serious inadequacies, but they represent significant steps forward, and additional models and better observations should lead to important advances.

Observationally, the investigation of mass loss and heating mechanisms using empirical modeling of cool giant atmospheres requires high-resolution profiles of key UV spectral lines. Some data of this type have been obtained during recent years with the *International Ultraviolet Explorer* (IUE) satellite. Spectra of many of the brightest red giant stars, including a few N-type carbon stars, have been obtained and analyzed in an exploratory way (Querci et al. 1982; Johnson & Luttermoser 1987). Seen at low resolution, the chromospheric emission in N stars appears weak and variable (Querci & Querci 1985; Johnson et al. 1988). However, a high-resolution IUE spectrum of TX Psc (N0: C6, 2) shows that the intrinsic chromospheric emission (in particular, Mg II *h* and *k* emission) is actually quite strong but badly mutilated by overlying circumstellar/interstellar absorption (Eriksson et al. 1986, hereafter EE86). Clearly, further high-resolution ultraviolet observations, such as will be presented here, are needed before we can learn more about the temperature and velocity structure of the chromospheres and address theoretical problems of mass loss in AGB stars.

The N-type carbon star UU Aur was chosen for this study not only for its brightness but also because it has been observed in many previous studies. For example, high-resolution spectra in the region 5050–7850 Å have been obtained for UU Aur and many other carbon stars by Barnbaum (1994). Furthermore, since it is not a Mira variable, its

properties, many of which are known, are not expected to vary greatly with time. An effective temperature of 2825 K has been obtained for UU Aur by the infrared flux method (Tsuji 1981). The angular diameter (over the wavelength range 7120–8000 Å) has also recently been measured by long-baseline visual interferometry to be  $11.28 \pm 0.21$  mas for a uniform disk (Quirrenbach et al. 1994). From broad-band photometry, a bolometric flux of  $\log f_{\text{bol}} = 5.546$  has been derived (Bergeat 1976; Tsuji 1981), which, when combined with the angular diameter measurement, yields an effective temperature of  $2767 \pm 25$  K, in good agreement with the results of the infrared flux method. Furthermore, the metallicity (Fe/H) has been shown to be solar within the errors of measurement, the  $^{12}\text{C}/^{13}\text{C}$  ratio is 52, and the C/O ratio is 1.06—all these values fall near the middle of the range for the 30 brightest N-type carbon stars (Lambert et al. 1986).

Absolute K magnitudes of N-type carbon stars in the Magellanic Clouds cluster rather tightly about the value  $-8.1$  (Frogel, Persson, & Cohen 1980; Bessell, Wood, & Lloyd Evans 1983). If one assumes this same value for UU Aur, the observed K magnitude of  $-0.71$  (Neugebauer & Leighton 1969) yields a distance of 300 pc. The star lies at  $l = 176^\circ.5$ ,  $b = +13^\circ.8$ , nearly opposite the direction to the Galactic center.

UU Aur was among the first carbon stars detected in both the 1–0 and 2–1 lines of CO and has been observed by several investigators, including team members (cf. Olofsson et al. 1993a). These authors find outflow velocities of CO (at 0.01–0.1 pc from the star) of  $11 \text{ km s}^{-1}$ , very similar to values observed for other carbon stars. With an estimate of the distance of about 300 pc, a mass-loss rate of  $1.3 \times 10^{-7} M_\odot \text{ yr}^{-1}$  is found, typical for N-type carbon stars (cf. van der Veen & Rutgers 1989; Olofsson et al. 1993a). However, they also find indications that this value might be an underestimate, perhaps a severe underestimate, of the true mass-loss rate.

Radio observations of HCN (1–0) emission and a limit on CS (2–1) emission were also obtained in an effort to compare elemental and isotopic abundances in circumstellar matter with those from the photosphere (Olofsson et al. 1993b). From the HCN measurements, these authors estimate an HCN abundance of the circumstellar envelope, relative to  $\text{H}_2$ , of  $2 \times 10^{-4}$ , which is typical of values for other carbon stars with similar mass-loss rates.

In a survey of N-type carbon stars at 3.6 cm with the VLA telescope, UU Aur was not detected at a flux upper limit of 0.070 mJy (Luttermoser & Brown 1992). In fact, no N-type carbon star was detected except V Hya, the lone Mira variable in the sample. From these upper limits, the authors deduced that non-Mira carbon stars cannot have chromospheric temperatures greater than 6000 K.

Below, we will describe spectral observations of UU Aur, concentrating on ultraviolet data from the *Hubble Space Telescope*. Line identifications and Doppler shifts will be reported and preliminary interpretations of the data will be offered. Further analysis will require detailed non-LTE semiempirical modeling of the chromosphere.

## 2. OBSERVATIONS AND DATA REDUCTION

Observations of the carbon star UU Aur (N3; C7, 2) were obtained by the *HST* on 1993 December 9. A low-resolution spectrum covering the region  $\lambda\lambda 2222\text{--}3275$  was taken with the Faint Object Spectrograph (FOS), while a high-resolution spectrum of the region near Mg II *h* and *k*,  $\lambda\lambda 2787\text{--}2833$ , was

obtained using the Goddard High Resolution Spectrograph (GHRS). The initial data reduction, calibration, and analysis of the *HST* observations were carried out by the GSFC/CSC members of the team (K. G. C. and R. D. R.).

In preparation for and to support the *HST* observations, ground-based, high-resolution spectra of UU Aur in the visual and near-infrared regions, including H $\alpha$  and the Ca II infrared triplet, were obtained in 1989 by D. G. L. and near the time of the *HST* observations by F. Q. and M. Q. These data will be described below. Additionally, members of our team have previously observed UU Aur in the ultraviolet at low resolution with *IUE* (Johnson & Luttermoser 1987) and at radio wavelengths (described above).

Throughout this paper we have assumed a heliocentric radial velocity for UU Aur of  $12 \text{ km s}^{-1}$ , obtained from optical measurements (Hoffleit & Jaschek 1982), and the wavelength scales in all plots have been adjusted to remove the corresponding redshift. Radio CO-line observations, which measure the motion of the center of mass of a very large circumstellar region, may provide the most accurate determination of the radial velocity, since there may be small, variable inflows and/or outflows in the photosphere. Values of radial velocity from various CO measurements for UU Aur range from  $10.6$  to  $14.7 \text{ km s}^{-1}$ , with an average of about  $13.5 \text{ km s}^{-1}$  (Barnbaum 1992b), while  $11 \text{ km s}^{-1}$  is recommended in a recent comprehensive paper (Olofsson et al. 1993a). The uncertainty in the radial velocity of UU Aur is likely less than  $\sim 2 \text{ km s}^{-1}$ .

### 2.1. The FOS Spectrum

A medium dispersion ( $R = 1300$ ) spectrum was obtained with the FOS instrument on the *HST* in 2.30 hr, yielding a resolution of  $\sim 0.5 \text{ \AA}$  ( $\lambda/\Delta\lambda = 1300$ ) and a signal-to-noise ratio that varies from about 30 at  $3200 \text{ \AA}$  to perhaps 5 at  $2800 \text{ \AA}$ , and even less at shorter wavelengths. Unfortunately, there was no calibration exposure done for this spectrum, so we have been forced to use the default calibration. This leaves an uncertainty of about  $1 \text{ \AA}$  in the wavelength scale.

The reduced FOS spectrum is presented in Figures 1 and 2. The line identifications are discussed in Section 3.1. In Figure 1, which shows the whole FOS spectrum on a compressed scale, one can see a gradual decrease in flux toward shorter wavelengths followed by a strong, broad rise at the shortest wavelengths. The short-wavelength increase in flux is due entirely to scattered light produced by the well-known red-leak in the FOS (HST Instrument Handbook 1994). However, the rise in flux toward the long-wavelength end of the spectrum is real, and atomic and molecular absorption features are superposed. Emission lines are obviously present throughout the spectrum.

### 2.2. The GHRS Spectrum

The raw data files for the GHRS spectrum were wavelength-calibrated using the explicit WAVE observations obtained along with the science data and transformed onto an absolute flux scale using the latest radiometric calibration of the GHRS. Software and techniques developed by the GHRS Instrument Definition Team were used to optimize these calibrations. The resolution ( $0.03 \text{ \AA}$ ) and signal-to-noise ( $\sim 10$ ) of this spectrum are much higher than for the FOS spectrum. The complete GHRS spectrum can be seen in Figure 3, and the Mg II *h* and *k* profiles are shown in detail in Figures 4 and 5.

### 2.3. Ground-based Observations

Ground-based observations of UU Aur in the optical, infrared, and radio have been made by members of our group in order to obtain additional clues concerning the nature of the star and its chromosphere. Here, we will present ground-based spectra of the H $\alpha$  and Ca II infrared triplet regions obtained by D. Luttermoser with the McMath-Pierce stellar spectrograph at Kitt Peak on 1989 February 11 (Fig. 6) and February 12 (Fig. 7), with resolutions of  $0.13$  and  $0.34 \text{ \AA}$ , respectively. M. and F. Querci have also observed these spectral regions, and although their observations were separated from those of Luttermoser by almost 5 years, the spectra are nearly identical.

## 3. ANALYSIS

The Indiana group (L. M. E. and H. R. J.) carried out the line identifications and the velocity analysis for the *HST* data. This information has been combined with velocities from visual and radio observations to try to obtain as complete a picture as possible of the velocity structure of the photospheric, chromospheric, and circumstellar regions. The temperature structure and ionization of the chromosphere can be obtained only by detailed spectral modeling, which will be described in a future paper.

### 3.1. The FOS Spectrum

As shown in Figure 1, the ultraviolet flux, outside of clear emission and absorption features, steadily decreases toward shorter wavelengths and reaches an apparent minimum value of  $\sim 5.5 \times 10^{-15}$  near  $2635 \text{ \AA}$ . The decrease in flux toward shorter wavelengths results from the swift decline of the Planck function and the mean intensity in the UV at the low temperatures of the continuum-emitting gas. If the temperature rise in the chromosphere is sharp enough to compensate for the quick falloff in the Planck function, and the densities in the region are great enough to form a continuum, one would be able to see the "continuum" (the true continuum is obscured by line blanketing) increase again toward shorter wavelengths. Observing a flux minimum, if one exists, would be important, since it would allow one to estimate the value of the temperature minimum at the base of the chromosphere. This information is practically nonexistent for very cool giants. However, one must not be tempted to identify the region of the flux minimum in Figure 1 as marking the temperature minimum, for essentially all the light shortward of  $2640 \text{ \AA}$  is actually scattered light from the red leak in the FOS. This scattered light also makes some contribution at the longer wavelengths.

In identifying the emission lines observed in the FOS spectrum (Fig. 2), we were guided by the high-resolution *IUE* spectrum of the M3-4 III star  $\gamma$  Cru (Wing, Carpenter, & Wahlgren 1983; Carpenter et al. 1988), recent GHRS observations of the M3 III star  $\mu$  Gem (Carpenter et al. 1994), the low-resolution *IUE* spectra of carbon stars (Johnson & Luttermoser 1987), and the single, high-resolution *IUE* spectrum of the N-type carbon star TX Psc (EE86). Rest wavelengths were obtained from *A Multiplet Table of Astrophysical Interest* (Moore 1959) and *An Ultraviolet Multiplet Table* (Moore 1962). Relative line intensities from the Multiplet Tables were also used to identify the strongest lines in each multiplet and hence aid in deciding which identifications to include in Figure 2.

In Figure 2 the most certain line identifications are indicated by symbols drawn at their rest wavelengths. The multiplet



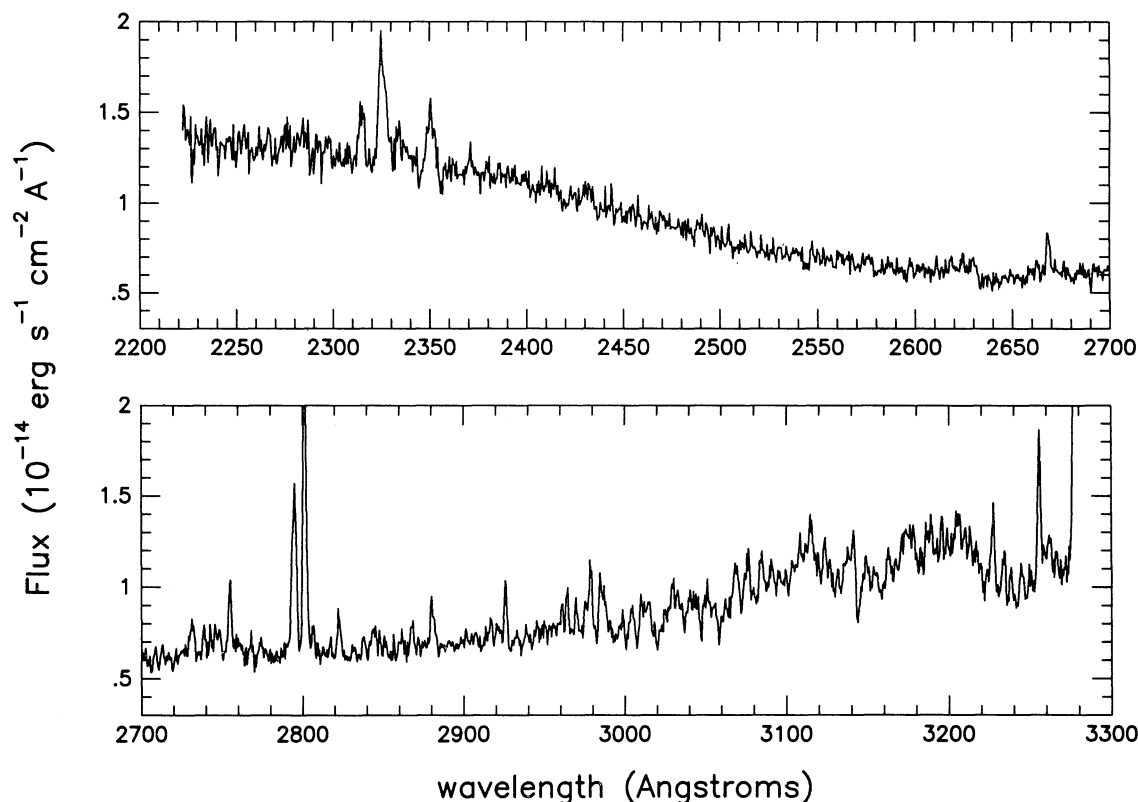


FIG. 1.—Complete FOS spectrum of UU Aur. The increase in flux toward the short-wavelength end of the spectrum is due to scattered light in the FOS detector.

designations corresponding to the different point types are listed in Table 1 in order of increasing wavelength. Because of the relatively low resolution and signal-to-noise ratio of the FOS spectrum, only the stronger lines of the multiplets can be identified with confidence. Weaker lines are often degraded and distorted by noise or blends with neighboring emission and absorption features. However, we believe, based on wavelength coincidences and comparisons between the FOS spectrum and GHRS spectra of  $\mu$  Gem, that most of the structure in the FOS spectrum reflects real underlying emission and absorption. Further advances in line identification must await higher-resolution observations.

The strongest identified emission lines are those expected from previous *IUE* observations and chromospheric models: Mg II *h* and *k*, the C II] lines at  $\sim 2325$  Å, Si II] lines at 2350 Å, Al II (UV1) at 2669 Å, and various lines of Fe II. The identification of emission from Fe II (UV1) rests not on the identification of individual lines but on the coincidence between the long-wavelength lines of this multiplet and an abrupt rise in the unresolved “pseudocontinuum.” No other identification seems reasonable. Fe II (UV62) is represented by strong lines at 2731, 2743, 2746 (blend with UV63), 2749 (partial blend with UV63), and 2756 Å. Fe II (UV63) shows lines at 2740 and 2747 (blend with UV62). Coincidences of other lines with spectral peaks occur but are suspect because stronger lines are absent. The intrinsically (cf. the *UV Multiplet Table*) strongest line of Fe II (UV60) appears at 2927 Å. The third, fourth, and (3) fifth strongest lines can be seen at 2971, 2979, 2940, 2961, and 2976 Å, respectively. The second strongest line, which lies at 2954 Å, is not obviously present in the data, but it could be washed out by a blend with an absorption line of Fe I (UV1) also at 2954 Å.

TABLE 1  
LINE IDENTIFICATIONS FOR FIGURE 2

| Symbol           | Multiplet Designation               |
|------------------|-------------------------------------|
| Emission Lines   |                                     |
| × .....          | C II (UV.01)                        |
| ▲ .....          | Si II (UV.01)                       |
| △ .....          | Fe II (UV1)                         |
| ☆ .....          | Al II (UV1)                         |
| △ .....          | Fe II (UV62)                        |
| × .....          | Fe II (UV63)                        |
| ○ .....          | Mg II (UV1) [ <i>h</i> & <i>k</i> ] |
| ✕ .....          | Fe I (UV45) Fl.?                    |
| * .....          | Fe II (UV399, 380, 391) Fl.         |
| ○ .....          | Fe I (UV44) Fl.                     |
| ☆ .....          | Mg I (UV1)                          |
| □ .....          | Fe II (UV61)                        |
| △ .....          | Fe II (UV60)                        |
| × .....          | Fe II (1)                           |
| Absorption Lines |                                     |
| * .....          | Fe I (9)                            |
| ● .....          | CH bandheads                        |

NOTES.—The multiplet designations are listed in order from shortest wavelength to longest wavelength, so that, although some symbols are used more than once, the correspondence between Table 1 and Figure 2 should be clear. Wavelengths of individual lines can be found in Moore 1962, 1959. “Fl.” marks fluoresced lines.

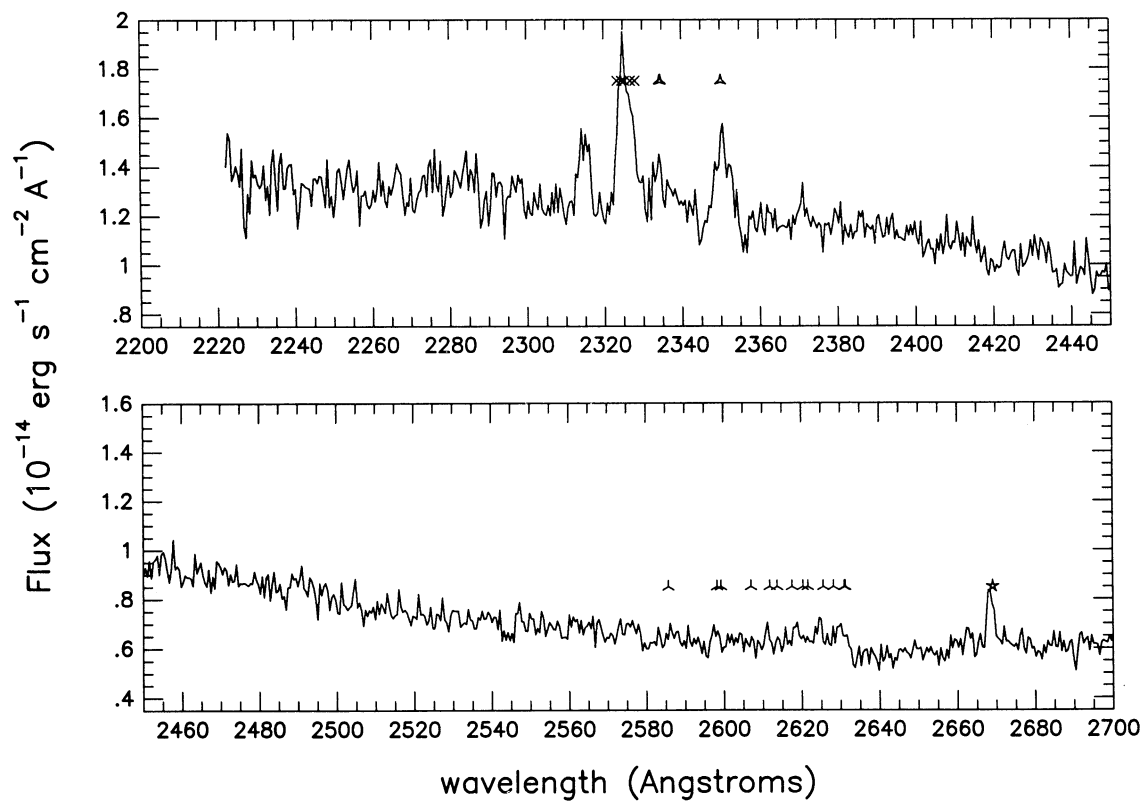


FIG. 2a

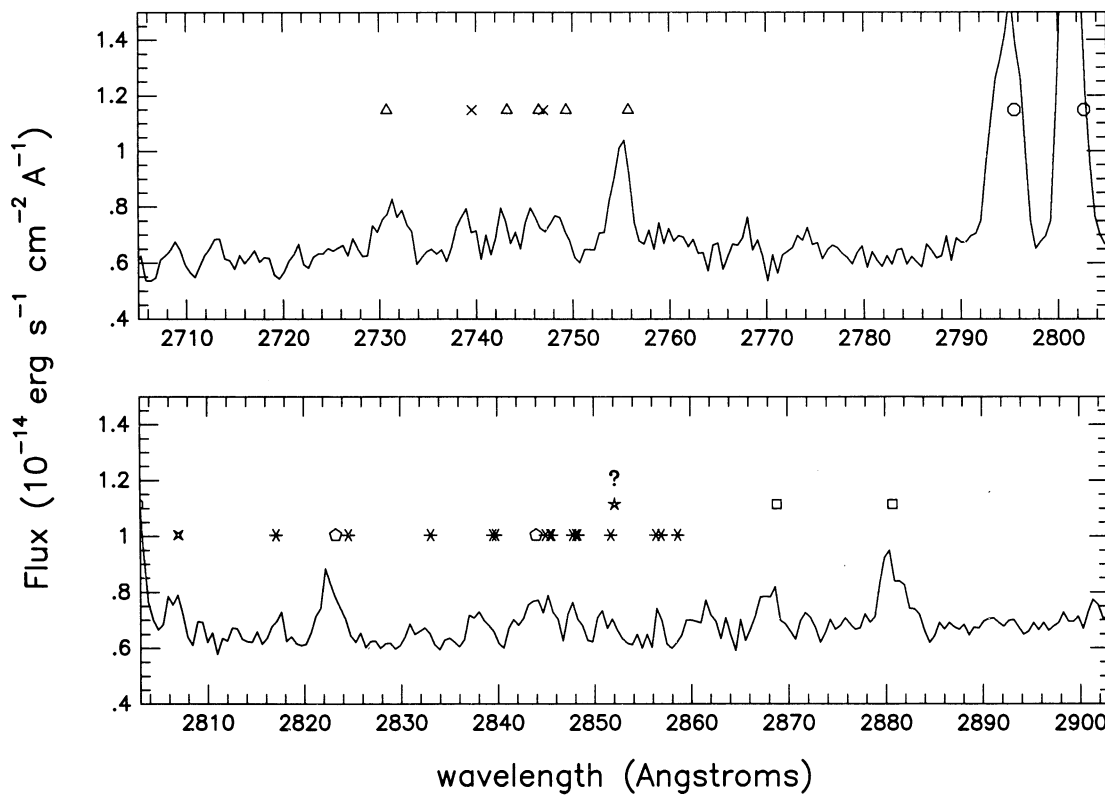
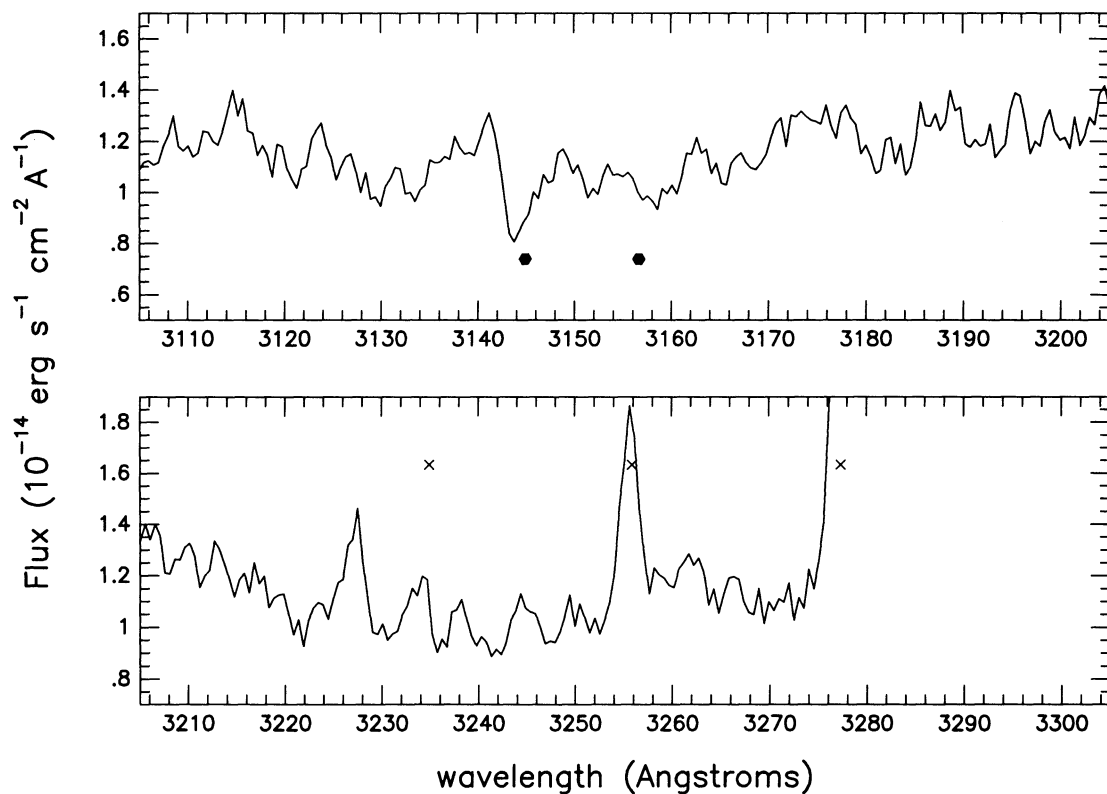
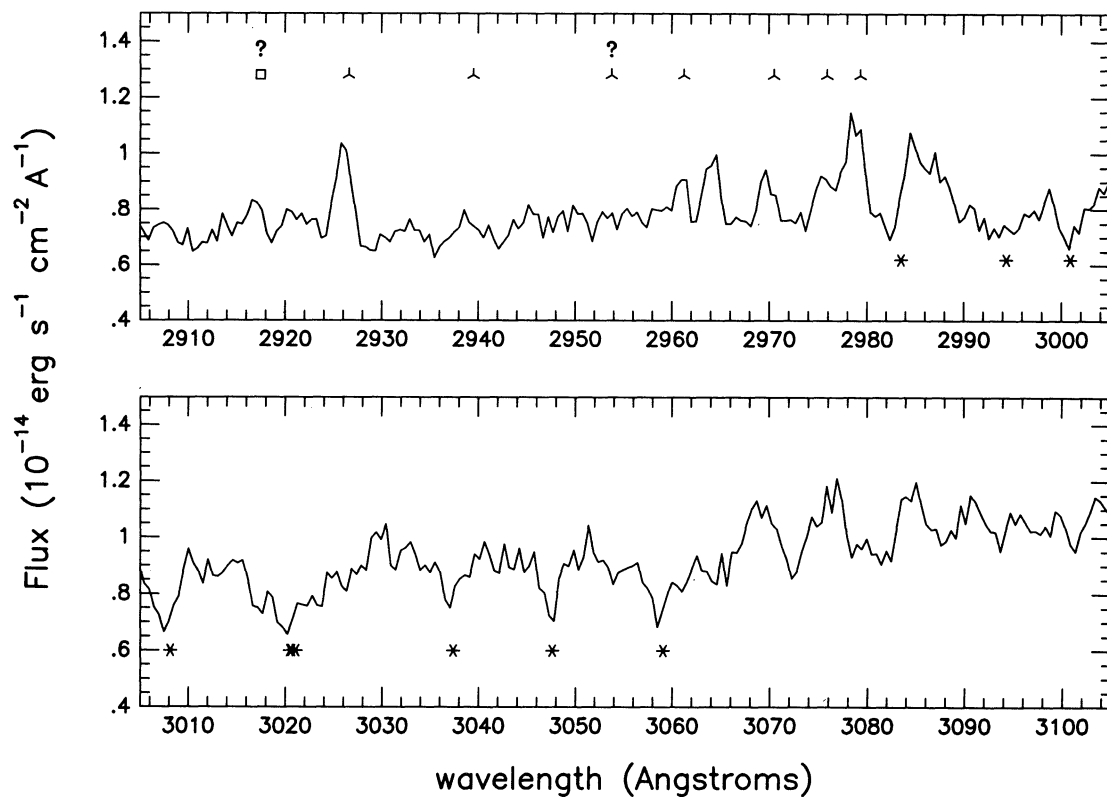


FIG. 2b

FIG. 2.—FOS spectrum of UU Aur. The symbols show rest wavelengths for the multiplets listed in Table 1. Emission lines are indicated by points above the spectrum, absorption lines by points below the spectrum.



There is other weak evidence for Fe I (UV1), but not enough to include it in our list of identified lines. Fe II (UV61) is represented by its strongest line at 2881, its next strongest at 2869, and perhaps another line at 2917 Å. The presence of Mg I at 2852 Å, an important diagnostic feature, is uncertain due to possible overlying interstellar and self-absorption and/or blending with fluorescent Fe II emission.

In addition to the lines identified in Figure 2, Fe II (6) is clearly seen at 3228 Å and probably also at 3213 Å. These two lines should have the same strength, and they do have roughly the same peak flux; only the background fluxes appear to be different. The weaker lines of the multiplet are not recognizable. The distinct peak at 3196 Å may be due to the strongest line of Fe II (7). The large peak at 3141 Å coincides with another line of Fe II (7), but the *Multiplet Table* lists its intensity as 0. Other lines are not recognizable, leaving the presence of this multiplet in doubt. Finally, Fe II (8) could also be present, the strongest two lines combining to give the peak at 2964 Å and the next two strongest blending to produce the peak at 2985 Å.

The largest remaining unidentified emission feature lies at 2315 Å. Some of the unidentified peaks between 2980 and 3280 Å may be emission lines, but some or most may simply be gaps between absorption features.

Several pumped (fluoresced) emission lines are also seen in the FOS spectrum. As expected, the Fe I (UV44) lines at 2823.28 Å ( $J_F J_u$ : 3-3) and 2843.98 Å (2-3), which are pumped by the Mg II  $k$  line through a line at 2795.54 Å (4-3) are present. The first is also present in the GHRS spectrum (see

Fig. 3). Several fluorescent emission lines of Fe II (UV 380, 391, and 399) between 2815 and 2860 Å, which are present in  $\gamma$  Cru (Carpenter et al. 1988), may also be present here, but individual lines cannot be distinguished.

A previously unobserved emission line is noted at 2807.0 Å. Although rather inconspicuous in the FOS spectrum just longward of the intense 2802 Å line of Mg II, it appears clearly as a narrow emission line in the GHRS spectrum (see Fig. 3). We tentatively identify this feature as fluoresced emission from the 2806.98 Å line of Fe I (UV45) (see § 3.3).

In the FOS spectrum there is no structure at all in the Mg II  $h$  and  $k$  profiles. The comparison of low- and high-resolution observations in Figure 3 shows dramatically how much structure is actually present and illustrates the difficulties in identifying lines and determining velocity shifts from spectra of low resolution. Without the benefit of the high-resolution GHRS spectra, one would have no knowledge of the existence of overlying absorption and might mistakenly underestimate the intrinsic chromospheric emission in UU Aur, as was noted in the similar carbon star TX Psc (EE86). At high resolution, the many Fe II lines present in the FOS spectrum might also show central self-absorption as they do in the cool giant  $\mu$  Gem (Carpenter et al. 1994).

Although the spectral resolution of the FOS spectrum is too low to allow reliable measurements of the wavelength shifts of individual lines, visual inspection reveals a systematic shortward shift of the emission lines by  $\sim 0.5$  Å. (Different lines have different shifts with different uncertainties, but the shifts are certainly not equally distributed around zero.) Only the Si II

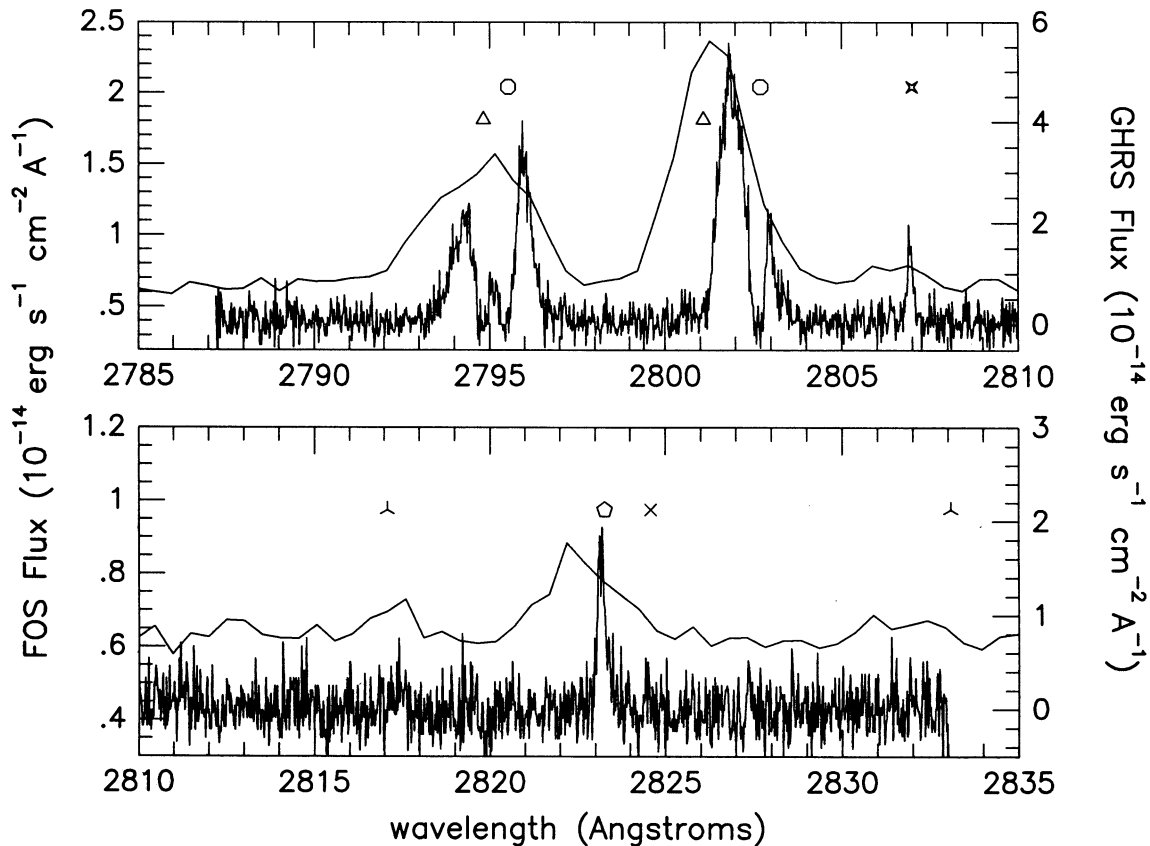


FIG. 3.—Overlay of the FOS and GHRS spectra showing the difference in resolution and a possible wavelength calibration error in the FOS spectrum. See Table 2 for line identifications.

TABLE 2  
LINE IDENTIFICATIONS FOR FIGURE 3

| Symbol           | Multiplet Designation                 |
|------------------|---------------------------------------|
| Emission Lines   |                                       |
| ○.....           | Mg II (UV1) [ <i>h</i> and <i>k</i> ] |
| ✕.....           | Fe I (UV45) Fl.?                      |
| λ.....           | Fe II (UV380) Fl.                     |
| ◇.....           | Fe II (UV44) Fl.                      |
| ×.....           | Fe II (UV399) Fl.                     |
| Absorption Lines |                                       |
| △.....           | Mn I (1)                              |

NOTE.—See Table 1 caption.

line at 2350 Å shows an apparent redshift (of 0.4 Å). If we neglect this line, the five largest, sharpest identified emission lines give an average blueshift of about 0.6 Å (individual values lie between 0.3 and 0.7 Å), where we have taken line center to lie at the “center of mass” of the line. Weaker, but relatively sharp, lines give an average blueshift of 0.7 Å (values from 0.2 to 1.0 Å).

A shift of 0.6 Å corresponds to a velocity of 62 km s<sup>-1</sup> at  $\lambda = 2900$  Å. However, the uncertainty in the wavelength scale is of the same order (0.5–1.0 Å), so the shifts may not reflect actual gas velocities in the chromosphere. An overlay of the FOS and GHRS data, where they coincide (Fig. 3), shows that there may, indeed, be an error of about 0.5 Å in the FOS wavelength calibration. The centroid of Mg II *h* in the FOS spectrum appears to be shifted shortward by at least 0.5 Å relative to its position in the GHRS spectrum, and the peak corresponding to Fe I (UV44) is shifted by about 1 Å, but the situation for Mg II *k*, Fe I (UV45), and Fe II (UV380) is less clear. Obviously, the low resolution of the FOS data can lead to spurious wavelength shifts due to undersampling of the profiles and to blending. Allowing for the uncertainties due to the low spectral resolution and the wavelength scale, it is possible (though not demonstrated) that velocities of several tens of km s<sup>-1</sup> were present in the chromosphere of UU Aur at the time these spectra were taken. Such velocities would be consistent with the overall shifts of the Mg II emission lines as determined from the high-resolution data (§ 3.2).

Due to their sharpness, semiforbidden and fluorescent lines could give excellent velocity information, especially since they may form in regions of the atmosphere different from other emission lines. Ratios of the C II] lines could also give electron density information. Unfortunately, in the FOS spectrum none of the five members of C II (UV0.1) group are resolved, nor are the members of the two groups of Si II] lines; any velocity shifts or line ratios are thus indeterminate. Similarly, no velocity information can be obtained from the fluorescent lines in the FOS spectrum. Observations of these lines with higher resolution would be extremely valuable. (The two fluoresced lines in our GHRS spectrum will be described below.)

Since this is the first spectrum of a carbon star with measurable continuous flux at short wavelengths (down to  $\sim 2600$  Å), one might also expect to trace photospheric absorption lines from neutral metals to shorter wavelengths than before. In fact, unmistakable absorption features due to Fe I (9) are seen down to 2900 Å (Fig. 2). A dip at 2720 Å might be due to a blend of the two strongest lines of Fe I (UV5), but the feature is no deeper than neighboring, unidentified dips at 2690 and 2708 Å

so we are hesitant to make the identification. Molecular absorption features may also be present in the FOS spectrum. Two dips coincide with bandheads of the “3143 system” of CH about 3145 and 3157 Å (Pearce & Gaydon 1963).

A few of the absorption features in the FOS spectrum lie at the wavelengths of known interstellar lines. This may be a coincidence, since interstellar lines are normally quite narrow and might not be expected to show at this resolution, but the distance to UU Aur is quite large (300 pc), and it lies near the Galactic plane, therefore interstellar lines may be rather strong. The strongest interstellar lines in our wavelength region are naturally Mg II *h* and *k*. These show up clearly in the GHRS data and will be discussed below. Next strongest, according to observations of Zeta Ophiuchi (Morton 1975), are Mg I  $\lambda 2852$  and five Fe II lines between 2343 and 2599 Å. There is no evidence for these Fe II lines in the spectrum of UU Aur, perhaps due to the low background flux and the noise at those wavelengths. Mg I absorption could be blended with chromospheric emission from the same transition and would not be visible at low resolution.

Absorption features also appear at the wavelengths corresponding to the stronger lines of Ti II (5) at 3088.0, 3078.6, 3075.2, and 3073.0 Å. Weaker features seem to coincide with the stronger lines of Ti II (10) as well. Although Ti II is the dominant ion of Ti in the interstellar medium (the 3073.0 Å line and three other Ti II lines outside our wavelength region are weak but present in the spectrum of Zeta Ophiuchi), it would be surprising if the lines in UU Aur were interstellar, for we would not expect them to be strong enough to be observed at this resolution. They might instead be formed in the chromosphere of UU Aur. Detailed modeling and high-resolution observations will be needed to unambiguously determine the source of these lines.

The Fe I (9) absorption lines have apparent blueshifts between 0 and 1.1 Å, with an average of 0.5 Å, about the same as the average shift of the strong emission lines. Velocities for other possible absorption features cannot be determined.

### 3.2. The GHRS Spectrum

The most interesting new data are the high-resolution GHRS profiles of the Mg II *h* and *k* lines. As can be seen in Figures 4 and 5, which show the data fitted with possible (nonunique) Gaussian emission profiles, there is strong chromospheric emission in these lines, but it is badly mutilated by a number of overlying absorption components. Such absorption is not unexpected given earlier high-resolution *IUE* observations of the carbon star TX Psc (EE86). However, the *HST* spectrum has a higher resolution and a much stronger signal than the *IUE* spectrum.

As expected, the emission component of Mg II *h* is narrower than that of Mg II *k*. The FWZI (full width at zero intensity) of *h* and *k* are  $\sim 3.4$  and 4.3 Å, respectively. Using the sample Gaussian fits, we can also estimate FWHM (full width at half-maximum) values of  $\sim 1.2$  and 1.4 Å and a ratio of peak fluxes of about 0.75, but the uncertainty in these values could be fairly large.

The GHRS spectrum clearly shows that the Mg II *h* and *k* emission is not centered at the rest wavelength of either line. Using the sample Gaussian fits shown in the plots to estimate the shifts, we find that the *k* line is shifted shortward by 40–50 km s<sup>-1</sup>, while the *h* line is shifted shortward by 50–60 km s<sup>-1</sup> (all velocities are relative to UU Aur, and we have assumed a radial velocity of 12 km s<sup>-1</sup>, unless otherwise noted; shortward



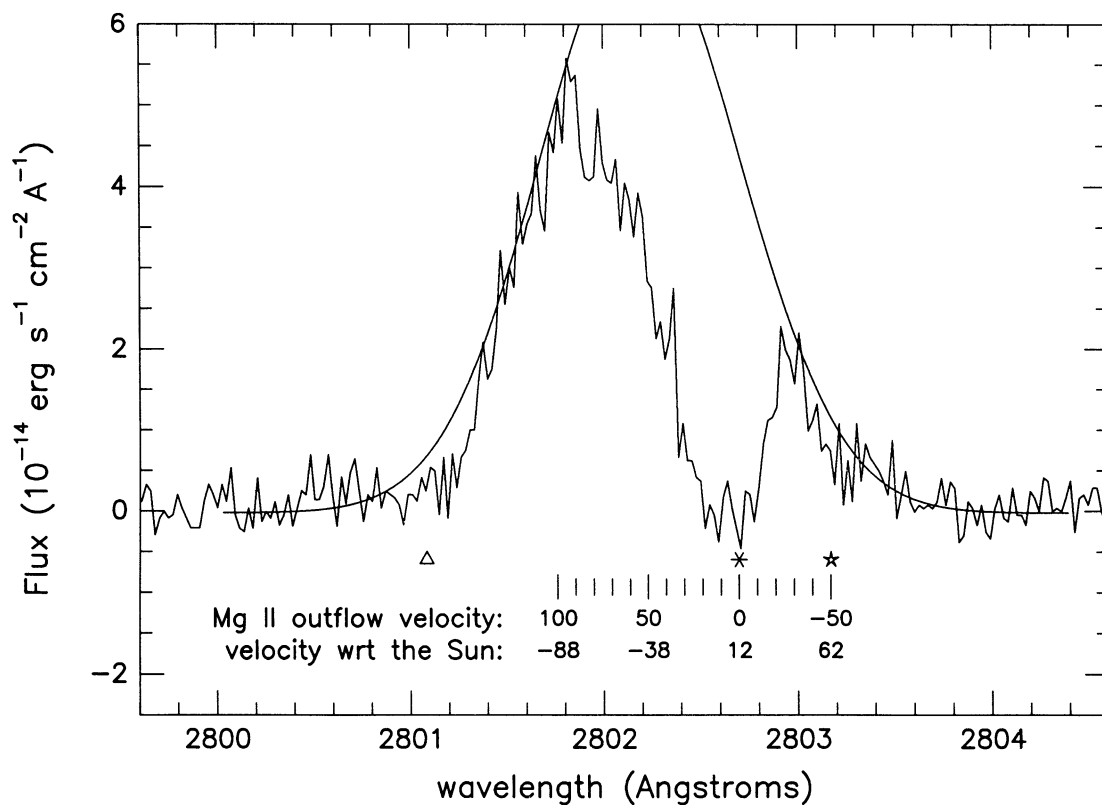


FIG. 4.—GHRS profile of Mg II *h*. Also shown is a possible Gaussian emission profile, centered at 2802.19 Å. The points show the rest wavelengths of Mg II *h* (asterisk), Mn I (UV1) (triangle), and Fe I (UV 3) (star). The velocity scales are for Doppler-shifted Mg II *h*—the upper numbers give velocities relative to UU Aur in  $\text{km s}^{-1}$  (positive = outflow); the lower numbers give heliocentric velocities for material lying between UU Aur and the Sun (positive = away from the Sun).

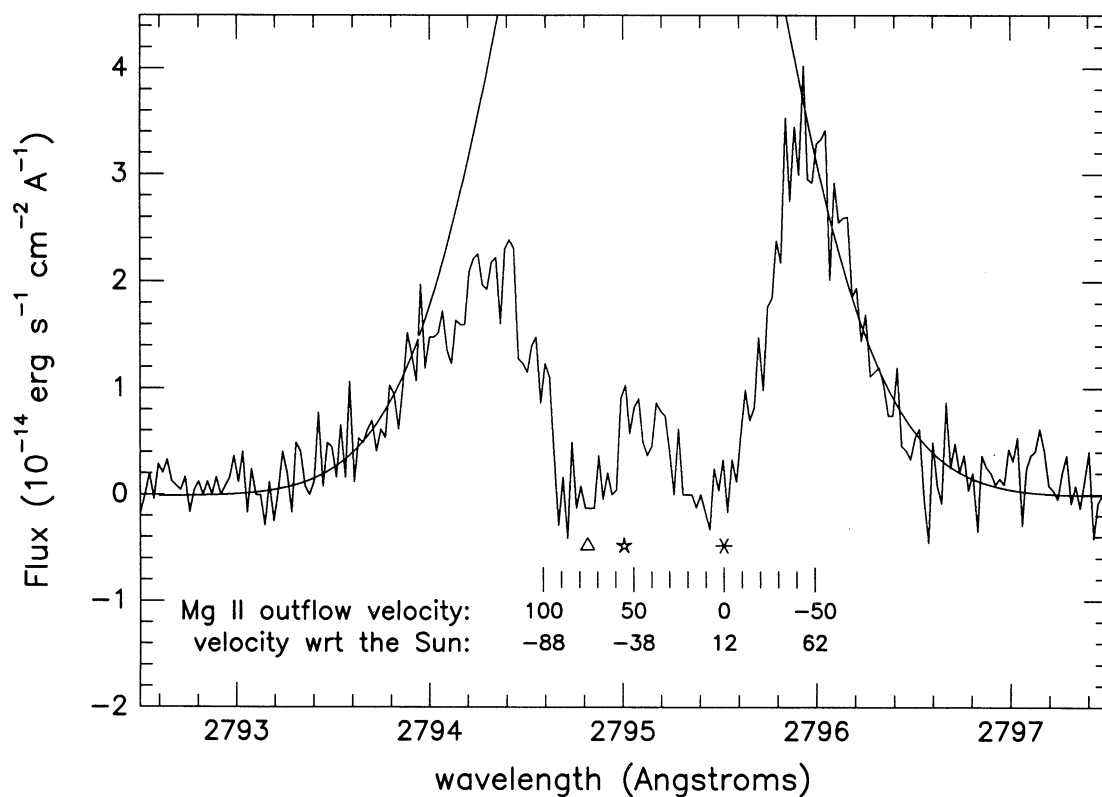


FIG. 5.—GHRS profile of Mg II *k*. A possible Gaussian emission profile, centered at 2795.10 Å, is also shown. See Fig. 4 caption for further information.

shifts = positive velocities relative to UU Aur = outflow). Because such strong emission lines are formed from contributions throughout the chromosphere, these velocities should be interpreted as rough global averages over the entire emitting region. Detailed chromospheric modeling must be done to obtain more detailed information.

Several types of absorption lines can be seen in the Mg II emission—chromospheric self-absorption, overlying circumstellar absorption, and absorption from interstellar clouds. In both Mg II profiles, there is a strong absorption feature centered about 0.1 Å shortward of the rest wavelength of the line (see Figs. 4 and 5). In our favored interpretation, this deep feature is self-absorption by matter in the upper chromosphere with an average outflow velocity of  $\sim 10 \text{ km s}^{-1}$ . If there is a velocity gradient through the chromosphere, there is no reason to expect the self-absorption to be centered in the emission profile.

In the  $k$  profile, there is a second strong absorption shortward of the first. This feature is centered at the rest wavelength of a Mn I (UV1) resonance line, and the simplest interpretation is that it is due to a stationary layer containing Mn I lying outside the region where the Mg II emission is formed; that is, circumstellar Mn I. (Interstellar Mn would presumably be ionized.) There is a second Mn I (UV1) resonance line in the shortward wing of the  $h$  profile, but since it occurs in a region with low flux, it is not as striking. The  $\log(gf)$  values for the two lines are 0.57 and 0.29, respectively, so that the line overlying Mg II  $k$  should for equal background fluxes, be almost twice as strong as that overlying Mg II  $h$ .

We can estimate the column density of the circumstellar envelope from the strength of the deep Mn I line overlying the  $k$  line. The optical depth of the absorbing layer is  $\tau_v = n(\text{lower}) a_v L$ , where  $\tau_v$  is the optical depth (here taken at line center),  $n(\text{lower})$  is the number density of atoms in the lower level of the transition,  $a_v$  is the atomic absorption coefficient (here taken at line center), and  $L$  is a scale length. To produce such a strong absorption line, the line-center optical depth must surely be greater than (and probably much greater than), say, 3, for which  $e^{-\tau} = 0.05$ . We recall that this line arises from the ground state ( $^6S_{5/2}$ ) of Mn I. The line-center absorption coefficient, for a temperature of 2000 K and a turbulent velocity parameter of  $2.0 \text{ km s}^{-1}$ , is  $1.2 \times 10^{-12} \text{ cm}^2/\text{atom}$ . An optical depth  $\tau \geq 3$  therefore requires a column density  $nL(\text{Mn I})$  of  $\geq 2.5 \times 10^{12} \text{ cm}^{-2}$ , where we assume that all Mn is Mn I and all Mn I is in the ground state. This value compares very well with the value obtained ( $> 1.4 \times 10^{12} \text{ cm}^{-2}$ ) by similar reasoning for TX Psc (EE86). Since the abundance of H is  $3 \times 10^6$  that of Mn (Anders & Grevesse 1989), the calculated column density of hydrogen in the circumstellar envelope of UU Aur is  $\geq 7.5 \times 10^{18} \sim 10^{19} \text{ cm}^{-2}$ . This is much smaller than the value suggested for cool giants with solar (oxygen-rich) envelopes (Tsuji 1988).

In addition to circumstellar Mn I, there is weak evidence for circumstellar Fe I. In the Mg II  $h$  profile, an Fe I (UV3) line lies in the longward wing. If the actual Mg II emission profile is similar to the one drawn in the figure, there is room for a weak Fe I absorption line with little or no outflow velocity. In the Mg II  $k$  profile, another Fe I (UV3) line lies nearer the center of the emission, but it is swamped by stronger absorption components. The  $\log(gf)$  values for these lines are  $-3.2$  ( $\lambda 2803.2$ ) and  $-2.2$  ( $\lambda 2795.0$ ) (Luttermoser et al. 1994), much smaller than those for the Mn I lines. The absorption features are much weaker and no additional information regarding column den-

sities can be gained from these lines. Note that the Fe I (UV3) line at 2795 Å is the pump transition for the strong fluoresced emission features of Fe I (42) at 4282 and 4308 Å that are seen in Mira-type variables (Bidelman & Herbig 1958). It would be interesting to see whether or not the fluoresced lines are also present in this non-Mira.

Absorption from gas clouds between the Earth and UU Aur must also affect the spectrum. Studies of the local interstellar (IS) medium have identified a nearby cloud moving at about  $+25 \text{ km s}^{-1}$  in the general galactic-anticenter direction (Böhm-Vitense 1981; Lallement & Bertin 1992). UU Aur lies quite close to the supposed boundary of this cloud and may lie behind it. If so, one would expect IS absorption at a heliocentric velocity of around  $+(20\text{--}25) \text{ km s}^{-1}$ , which corresponds to a velocity of about  $-8$  to  $-13 \text{ km s}^{-1}$  relative to UU Aur. (Note that we take positive velocities to denote motion away from the reference point, so, an IS cloud lying between UU Aur and the Sun, moving at  $+25 \text{ km s}^{-1}$  relative to the Sun, would have a velocity of  $-13 \text{ km s}^{-1}$  relative to UU Aur, whereas a similar cloud lying beyond UU Aur would have an velocity of  $+13 \text{ km s}^{-1}$  relative to UU Aur. In Figures 4 and 5, a scale indicating where the Mg II line would lie for various outflow velocities is included, along with a scale showing the corresponding velocity with respect to the Sun for outflowing gas or interstellar clouds lying between UU Aur and the Sun.) We thus place IS absorption near the centers of the Mg II  $h$  and  $k$  emission profiles, above the small central emission bump in the  $k$  line and at the sharp drop in flux in the  $h$  line.

Since the distance to UU Aur is quite large ( $\sim 300 \text{ pc}$ ), other interstellar Mg II components may also be present, probably at similar or smaller velocities since interstellar clouds usually have relatively small peculiar velocities and galactic rotation would not introduce any large relative motions at  $l \sim 180^\circ$ . No such absorption is obvious in the data, but, without detailed modeling or observations of a star very near UU Aur, one cannot say for certain whether other IS components exist or where their absorption features might lie. Given this uncertainty, we cannot say for certain that the absorption identified as self-absorption is not wholly or partially interstellar, or that the self-absorption might lie elsewhere in the profile.

In addition to Mg II  $h$  and  $k$ , the GHRs spectrum contains two fluoresced emission lines of Fe I. The Fe I (UV44) line at 2823 Å is shifted by  $5\text{--}15 \text{ km s}^{-1}$ , while the line at 2807 Å, if it is Fe I (UV45) (see § 3.3), is shifted by  $2\text{--}8 \text{ km s}^{-1}$ . The uncertainties arise from the difficulty in locating the line center in the face of noise and line asymmetries. Still, the fact that these velocities are so much lower than those of the Mg II emission indicates a region of formation outside the bulk of the Mg II-emitting region (the chromosphere). This circumstance contrasts strikingly with that in K-giant stars, in which it has been deduced from radiative-transfer calculations that the fluoresced Fe I (UV44) lines are formed in the chromosphere itself (Harper 1990). In the case of UU Aur, it seems likely that the fluorescent lines are formed in or above the upper chromosphere, especially if our proposed mechanism for pumping Fe I (UV45) is correct.

### 3.3. Fe I (UV45)

As mentioned above, we have tentatively identified the emission feature at 2807 Å, seen in both the FOS and GHRs spectra, as Fe I (UV45). The transition from the  $a^5F_4$  state to  $z^5H_5^o$  lies at 2806.98 Å. If this identification is correct, we need

to explain how the upper state could be populated. Collisional processes are unlikely, since other lines of the same multiplet with similar laboratory intensities show no evidence of emission. Also, lines of Fe I generally do not appear in the UV emission spectra of late-type stars unless excited by fluorescence, as in the case of the Fe I (UV44) lines. Thus we must look for a pump. Only one other line in the *Ultraviolet Multiplet Table* has the same upper state, namely the line at 2772.1 Å of the same multiplet. In our FOS spectrum there is nothing obvious at that wavelength which could serve as a pump. However, the  $z^5H^\circ$  state should combine with the  $a^5D$  ground state, and in fact it does through multiplet UV13, although, strangely, only one line of this multiplet is listed in the *Ultraviolet Multiplet Table*.

Since the most effective pumps are those that raise an atom from its ground state, we calculated the wavelength of the 4–5 transition of multiplet UV13, raising Fe I from its true ground state (0.00 eV) to the upper state of the 2807 Å line. Since the term value of the  $z^5H^\circ_3$  state is  $42991.66 \text{ cm}^{-1}$ , the wavelength in air of the transition is 2325.32 Å. This is almost precisely the wavelength of the strongest line (2325.40 Å) of multiplet UV0.01 of C II which is, after the Mg II doublet, the strongest emission feature seen in our FOS spectrum of UU Aur! We propose, then, that neutral Fe in the ground state absorbs photons from the C II] 2325.4 Å line and reradiates some of the energy at 2807.0 Å. This mechanism should also produce emission at 2772.1 Å, and it would be desirable to look for that line at high resolution. Should this fluorescence mechanism be accurate, the appearance of Fe I (UV45) at 2807 Å will be very sensitive to the velocity difference between the chromospheric and circumstellar gas due to the thinness of the C II line. As this velocity difference changes with time, Fe I (UV45) may disappear and reappear over time. This may explain why there is no evidence of 2807.0 Å emission in our *IUE* spectrum of TX Psc. An attractive feature of this mechanism is that it should operate wherever strong C II] emission shines through cool gas, as in the circumstellar shells of carbon stars. Note that the gas producing the 2807 Å emission may actually be quite cold, since the absorbing atoms are in their lowest state. It will be of considerable interest to search for this line in the ultraviolet spectra of M giants and supergiants.

### 3.4. Ground-based Observations

H $\alpha$  emission has been seen in carbon stars which are Mira-type variables (Barnbaum 1994); in fact, the appearance of H $\alpha$  in emission is often taken as the signature of a Mira variable. As can be seen in Figure 6, there is no evidence for strong H $\alpha$  in UU Aur, either in emission or absorption, although a weak H $\alpha$  feature could be hidden among the forest of CN lines that dominate the spectrum. The weakness (or absence) of H $\alpha$  in this star is consistent with its SRb subtype (Barnbaum 1992b, 1994) and provides a strong constraint for chromospheric models (LJAL).

The spin-forbidden transition of Ca I (1) at 6572.781 Å, also indicated in Figure 6, lies near the H $\alpha$  line. Since the oscillator strength is small for this line, we can be assured that it forms in the photosphere. If the radial velocity of UU Aur is  $12.0 \text{ km s}^{-1}$ , then the portion of the photosphere producing this line must be *inflowing* slightly at about  $3 \text{ km s}^{-1}$ .

Like the H $\alpha$  region, the near-IR in the Ca II (2) region is heavily blanketed by CN lines. However, two of the three Ca II lines, which lie at 8498.023, 8542.091, and 8662.141 Å (R. L. Kurucz, private communication 1994), are clearly seen as the

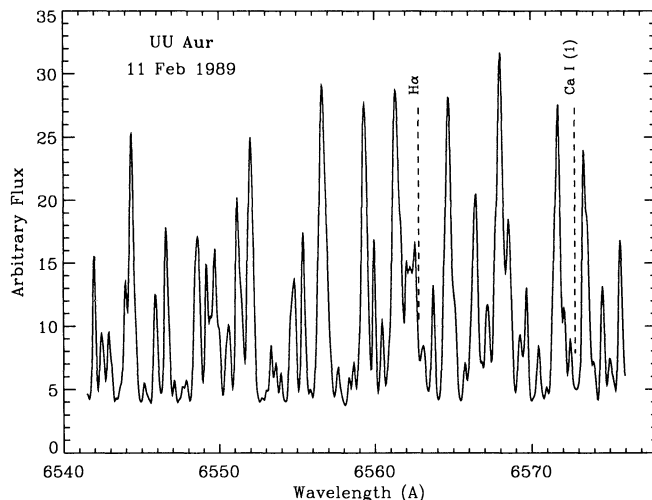


FIG. 6.—Spectrum of UU Aur in the region of H $\alpha$ . The rest wavelengths of H $\alpha$  and the Ca I (1) spin-forbidden transition have been labeled.

deepest troughs. These features, whose rest-frame locations are marked in Figure 7, show an *inflow* velocity of  $11 \pm 1 \text{ km s}^{-1}$  relative to the photosphere. If the cores of these lines form in the lower chromosphere, as was the case in the LJAL model for TX Psc, this inflow presents a sharp contrast to the velocity of the Mg II *h* and *k* emission features, which also form in this region but show an outflow.

### 4. VARIABILITY

Two issues that make the problem of chromospheric velocities more interesting, but more confusing, are time dependence and spatial inhomogeneities. Although UU Aur is not highly variable, small velocity changes in the photosphere and chromosphere probably occur, and spatial inhomogeneities (“spots,” circulation patterns, etc.) could also exist. Evidence for both is slowly accumulating, but they cannot be properly addressed or disentangled with the limited number of observations now available.

Time dependence in photospheric absorption lines has been found by Barnbaum (1992a), who obtained high-resolution

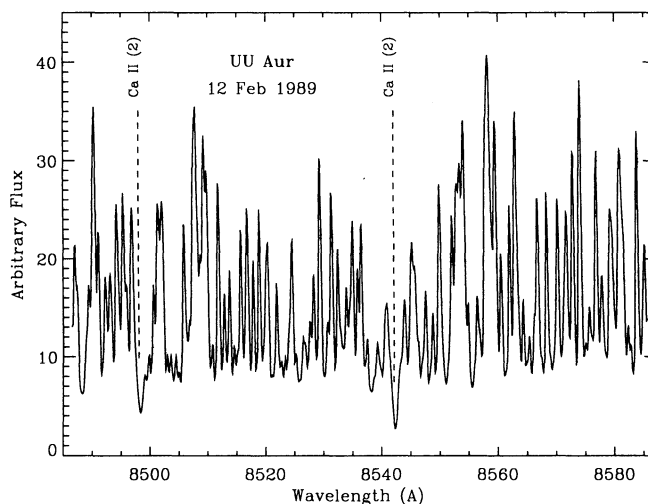


FIG. 7.—Near-IR spectrum of UU Aur. Rest wavelengths of two of the Ca II (2) infrared triplet lines have been marked.



spectra of UU Aur on two occasions, 1 year apart (1989 Dec. 10 and 1990 Dec. 9). A cross-correlation against the spectrum of TX Psc found an average inflow of 4.5 and  $1.3 \pm 2$  km s<sup>-1</sup> for the CN-dominated spectrum on the two dates. She also measured lines of Mg I (5183 Å), Li I (6708 Å), and K I (7699 Å); with respect to the rest frame of UU Aur these velocities were -6.9/-1.2, -0.8/3.2, and  $7.9/6.0 \pm 1.5$  km s<sup>-1</sup>, respectively, for 1989/1990 (positive = outflow; assuming a radial velocity of 12 km s<sup>-1</sup>). Data for other SRb carbon stars reveal that variations of a few km s<sup>-1</sup> around 0 are common, while Miras show much larger variations. Still, data for any given date hint at a gradual acceleration through the outer photosphere. Spectral modeling is needed to determine the depth of formation of each line and whether there is a smooth transition from inflow to outflow as radius increases. If modeling cannot explain the (changing) velocity structure in a consistent manner, spatial inhomogeneities—regions of outflow interspersed with regions of inflow—may have to be invoked in the photosphere as they have been for the chromosphere of the giant 30 g Her (Luttermoser et al. 1994).

Variability in the strength of chromospheric emission from the carbon star TX Psc has been discussed by Johnson et al. (1986). The resolution of the observations was insufficient to observe velocity variations, but it seems reasonable to expect some variation there as well. They found that the integrated flux of the blended Mg II *h* and *k* lines varied by at least a factor of 8 and that of the C II] lines by at least a factor of 5 within a 3 yr period.

## 5. CONCLUSIONS

In this paper, we have presented the first *HST* spectra of the chromosphere of a carbon star, UU Aur. Two spectra have been obtained—a lower resolution FOS spectrum covering about 1100 Å in the UV and a higher resolution GHRS spectrum spanning about 40 Å around the *h* and *k* lines of Mg II. We have also presented ground-based spectra of the regions around H $\alpha$  and the Ca II infrared triplet.

Despite the poor spectral resolution, uncertain wavelength calibration, and low signal-to-noise ratio of the FOS spectrum, we have been able to identify emission lines of C II, Mg I, Mg II, Al II, Si II, and Fe II. Weaker lines are probably present but cannot be identified beyond question. Fluoresced emission lines from Fe I are also present, as well as Fe I photospheric absorption. The stronger emission lines, as well as the Fe I absorption, appear to be shifted shortward by  $\sim 0.5$  Å, on average. If there were no uncertainties in the wavelength calibration, we would infer velocities of several tens of km s<sup>-1</sup> in the chromosphere, and such velocities would be consistent with the results from the GHRS spectrum. However, the uncertainty in the FOS wavelength scale is of the same order, and further observations are required before any definite claims can be made.

In the GHRS spectrum, the prominent Mg II lines show much structure and overall, shortward wavelength shifts that correspond to 40–60 km s<sup>-1</sup>. These large shifts indicate that similar velocities or velocity gradients exist in the chromosphere. Self-absorption, Mn I circumstellar absorption, and Mg II interstellar absorption overlie the Mg II *h* and *k* chromospheric emission. We have placed the self-absorption at about +10 km s<sup>-1</sup> relative to the surface of UU Aur, the Mn I near 0 km s<sup>-1</sup> with respect to the same surface, and the IS absorption at about +20–25 km s<sup>-1</sup> with respect to the Sun. Although without detailed modeling, we cannot distinguish the self-

absorption and the IS absorption with certainty, for now we adopt this simplest solution.

We have also noted the presence of a previously unobserved line at 2807 Å, which we attribute to fluorescence of Fe I (UV45). A mechanism has been proposed by which this line is pumped by one of the strong C II] emission lines.

A tentative picture of the velocity structure of the upper photosphere and chromosphere thus emerges. Deep under the photosphere, velocities must be very small, but already at photospheric levels, time-dependent motion is apparent. Absorption lines (of CN, Mg I, K I, and Li I) show inflow and outflow velocities of a few km s<sup>-1</sup> (Barnbaum 1992a). It is tempting to assume that these are the result of a gradual acceleration through the upper photosphere, though this remains to be proven by detailed modeling. It is also clear that the velocity structure in these layers is not stable (Barnbaum 1992a, b) in either magnitude or direction. Likewise, we have reported here that the Ca I spin-forbidden line at 6573 Å (presumably formed in the photosphere) and the Ca II infrared triplet lines (probably formed at the base of the chromosphere) arise in inflows of about 3 and 11 km s<sup>-1</sup>, respectively, in contrast to the general outward motion of the bulk of the chromosphere. There is evidence from Mg II for outflow velocities of order 40–60 km s<sup>-1</sup> in the chromosphere itself (at the time of our *HST* observations). At the top of the chromosphere, where the Mg II self-absorption arises, the velocity seems to have fallen back to about 10 km s<sup>-1</sup>. Fluorescent Fe I (UV44) emission is also shifted shortward by about 10 km s<sup>-1</sup> and Fe I (UV45) by 2–8 km s<sup>-1</sup>. Neutral iron could lie above the chromosphere or at the temperature minimum. If our proposed pumping mechanism for Fe I (UV45) works, it must lie exterior to the C II]–emitting region, thus most likely at or beyond the top of the chromosphere. At that same layer or at an even greater distance in a cool circumstellar envelope, Mn I, and perhaps more Fe I, is nearly at rest. Circumstellar CO (which is observed at a radius of 0.01–0.1 pc) is expanding at about 10 km s<sup>-1</sup>. (Table 3 gives a summary of this velocity information.)

Clearly, the outer atmosphere of UU Aur has a complex velocity structure. On a large scale, faster moving material is found between layers of slower moving material, implying that acceleration is taking place and a shock must eventually form (if it has not already). Is there other evidence for outflows or shocks? In the only available chromospheric model for a carbon star (TX Psc: LJAL), a shocklike velocity structure was necessary to place the calculated Mg II *h* and *k* lines exactly over the observed lines from an *IUE* high-resolution spectrum. (From the photosphere outward, the inferred velocity rose steeply from 0 to 50 km s<sup>-1</sup>; it then dropped more slowly and leveled off at 1 km s<sup>-1</sup>.) While the low signal of the *IUE* spectrum did not put the reality of that high-velocity outflow beyond question, the present observations seem to show a similar outflow in the lower chromosphere of UU Aur. To put this in perspective, we note that the sound velocity in a gas at 6000 K is about 8 km s<sup>-1</sup>. An outflow speed of 40 km s<sup>-1</sup> is a flow at mach 5, and a speed of 60 km s<sup>-1</sup> is close to mach 8. This strongly suggests that *hydrodynamic* and not hydrostatic processes dominate the structure of the lower chromosphere in these stars.

The existence of simultaneous inflows and outflows may indicate spatial inhomogeneities or large-scale circulations in the atmosphere as occur in some M stars (Carpenter et al. 1994). Inhomogeneities have in fact also been suggested to resolve the discrepancy between Mg II and CO observations at the same height in the carbon star TX Psc (Jørgensen &



TABLE 3  
INFLOW AND OUTFLOW VELOCITIES IN THE ATMOSPHERE OF UU Aur

| Line   | Velocity <sup>a</sup><br>(km s <sup>-1</sup> ) | Flow Direction              | Spectrum <sup>b</sup> | References <sup>c</sup> |
|--|--|-----------------------------|-----------------------|-------------------------|
| Ca II IR triplet absorption .....                              | 11   | Inflow                      | IR                    | HST94                   |
| Mg I absorption (photosphere) .....                            | 7/1 <sup>d</sup>                               | Inflow                      | Optical               | Barnbaum 1992a          |
| CN absorption (photospheric) .....                             | 4.5/1.5 <sup>d</sup>                           | Inflow                      | Optical               | Barnbaum 1992a          |
| Ca I (I) absorption (photospheric) .....                       | 3  | Inflow                      | Optical               | HST94                   |
| Li I absorption (photospheric) .....                           | 1/3 <sup>d</sup>                               | Inflow/outflow <sup>d</sup> | Optical               | Barnbaum 1992a          |
| K I absorption (photospheric) .....                            | 8/6 <sup>d</sup>                               | Outflow                     | Optical               | Barnbaum 1992a          |
| Mg II <i>k</i> emission .....                                  | 40–50 <sup>e</sup>                             | Outflow                     | High-resolution       | HST94                   |
| Mg II <i>h</i> emission .....                                  | 50–60 <sup>e</sup>                             | Outflow                     | High-resolution       | HST94                   |
| Permitted emission .....                                       | ~60–65 average <sup>f</sup>                    | Outflow                     | Low-resolution        | HST94                   |
| Fe I absorption .....  | ~50 average <sup>f</sup>                       | Outflow                     | Low-resolution        | HST94                   |
| Mg II <i>h</i> and <i>k</i> self-absorption .....              | 10   | Outflow                     | High-resolution       | HST94                   |
| Fe I (UV44) fluorescent emission .....                         | 5–15   | Outflow                     | High-resolution       | HST94                   |
| Fe I (UV45) fluorescent emission .....                         | 2–8  | Outflow                     | High-resolution       | HST94                   |
| Mn I absorption (circumstellar) .....                          | 0  | ...                         | High-resolution       | HST94                   |
| CO (circumstellar) .....                                       | 10–15  | Outflow                     | Radio                 | See text                |
| Mg II <i>h</i> and <i>k</i> absorption<br>(Interstellar) ..... | 20–25<br>With respect to the Sun               | ...                         | High-resolution       | HST94                   |

<sup>a</sup> Velocities are obtained assuming a radial velocity of 12 km s<sup>-1</sup> for UU Aur.

<sup>b</sup> Low-resolution = FOS spectrum; high-resolution = GHRS spectrum.

<sup>c</sup> HST94 refers to the present paper.

<sup>d</sup> Velocities have been rounded to the nearest 0.5 km s<sup>-1</sup>, and values are given for two dates, one year apart, see text.

<sup>e</sup> This value represents an average for the entire region of line formation.

<sup>f</sup> Lines display a range of shifts from 0 to 1 Å (0–100 km s<sup>-1</sup>). Some are real, others are the result of blends. Part or all of the measured velocity may also be due to a wavelength calibration error. See text.

Johnson 1991) and as a possible solution to difficulties in matching both the Mg II emission and the C II] emission in 30 g Her (M6 III) with a one-component, NLTE chromosphere (Luttermoser et al. 1994). Finally, temporal variations in the velocity field, which have been observed at the photospheric level in UU Aur, and presumably occur in the chromosphere as well, are probably contributing to the apparent complexity. This would not be unexpected since UU Aur is an SRb variable star. A series of high-resolution observations over time is needed to disentangle all the possible motions.

Careful empirical NLTE modeling of the chromospheric temperature and velocity structure will be undertaken to confirm and expand upon the interpretations discussed above.

This research was supported by NASA through STScI grant GO 4685.

*Note Added in Manuscript.*—The calculated Fe I line at 2325.32 Å, which coincides with a C II] emission line and serves as the pump in our proposed mechanism for exciting the observed fluorescent line at 2807.0 Å, has recently been observed by G. Nave, S. Johansson, R. C. M. Learner, A. P. Thorne, and J. W. Brault (ApJS 94, 221 [1994]). Multiplet UV13 now has four measured lines and is multiplet 23 in the new numbering scheme of Nave et al.

#### REFERENCES

- Anders, E., & Grevesse, N. 1989, *Geochim. Cosmochim. Acta*, 53, 179  
 Barnbaum, C. 1992a, *AJ*, 104, 1585  
 ———. 1992b, *ApJ*, 385, 694  
 ———. 1994, *ApJS*, 90, 317  
 Bergeat, J., Sibille, F., Lund, M., & Lefevre, J. 1976, *A&A*, 52, 222  
 Bessell, M. S., Wood, P. R., & Lloyd Evans, T. 1983, *MNRAS*, 202, 59  
 Bidelman, W. P., & Herbig, G. H. 1958, *PASP*, 70, 451  
 Böhm-Vitense, E. 1981, *ApJ*, 244, 503  
 Bowen, G. H. 1988, *ApJ*, 329, 299  
 Bowen, G. H., & Willson, L. A. 1991, *ApJ*, 375, L53  
 Carpenter, K. G., Pesce, J. E., Stencel, R. E., Brown, A., Johansson, S., & Wing, R. F. 1988, *ApJS*, 68, 345  
 Carpenter, K. G., Robinson, R. D., Johnson, H. R., & Ensmann, L. M. 1994, *BAAS*, 26, 863  
 Cuntz, M., Rammacher, W., & Ulmschneider, P. 1994, *ApJ*, 432, 690  
 Eriksson, K., Gustafsson, B., Johnson, H. R., Querci, F., Querci, M., Baumert, J. H., Carlsson, M., & Olofsson, H. 1986, *A&A*, 161, 305 (EE86)  
 Frogel, J. A., Persson, S. E., & Cohen, J. G. 1980, *ApJ*, 239, 495  
 Gustafsson, B., & Jørgensen, U. G. 1994, *A&AR*, in press  
 Gustafsson, B., & Plez, B. 1992, in *Instabilities in Evolved Super and Hypergiants*, ed. C. de Jager & H. Nieuwenhuijzen (Amsterdam: North Holland), 86  
 Harper, G. M. 1990, *MNRAS*, 243, 381  
 Hoffleit, D., & Jaschek, C. 1982, *The Bright Star Catalogue* (4th ed.; New Haven: Yale University Observatory)  
 Johnson, H. R. 1991, *A&A*, 249, 455  
 Johnson, H. R., Baumert, J. H., Querci, F., & Querci, M. 1986, *ApJ*, 311, 960  
 Johnson, H. R., Eaton, J. A., Querci, F., Querci, M., & Baumert, J. H. 1988, *A&A*, 204, 147  
 Johnson, H. R., & Luttermoser, D. G. 1987, *ApJ*, 314, 329  
 Jørgensen, U. G., & Johnson, H. R. 1991, *A&A*, 244, 462  
 ———. 1992, *A&A*, 265, 168  
 Judge, P. G., & Stencel, R. E. 1991, *ApJ*, 371, 357  
 Knapp, G. R. 1986, *ApJ*, 311, 731  
 Lallemet, G. H., & Bertin, P. 1992, *A&A*, 266, 479  
 Lambert, D. L., Gustafsson, B., Eriksson, K., & Hinkle, K. H. 1986, *ApJS*, 62, 373  
 Luttermoser, D. G., & Brown, A. 1992, *ApJ*, 384, 634  
 Luttermoser, D. G., Johnson, H. R., Avrett, E. A., & Loeser, R. 1989, *ApJ*, 245, 543 (LJAL)  
 Luttermoser, D. G., Johnson, H. R., & Eaton, J. A. 1994, *ApJ*, 422, 351  
 Moore, C. E. 1959, *A Multiplet Table of Astrophysical Interest*, National Bureau of Standards Technical Note 36  
 ———. 1962, *An Ultraviolet Multiplet Table*, Circular of the National Bureau of Standards 488, Section 4  
 Morton, D. C. 1975, *ApJ*, 197, 85  
 Neugebauer, G., & Leighton, R. B. 1969, *Two Micron Sky Survey*, NASA Spec. Publ. 3047  
 Olofsson, H., Eriksson, K., Gustafsson, B., & Carlstrom, U. 1993a, *ApJS*, 87, 267  
 ———. 1993b, *ApJS*, 87, 305  
 Pearce, R. W. B., & Gaydon, A. G. 1963, *The Identification of Molecular Spectra* (New York: Wiley), 101  
 Querci, F., & Querci, M. 1985, *A&A*, 147, 121

- Querci, F., Querci, M., Wing, R. F., Cassatella, A., & Heck, A. 1982, *A&A*, 111, 120  
Quirrenbach, A., Mozurkewich, D., Hummel, C. A., Buscher, D. F., & Armstrong, J. T. 1994, *A&A*, 285, 541  
Rammacher, W., & Cuntz, M. 1991, *A&A*, 250, 212  
Sedlmayr, E. 1994, in *Molecules in the Stellar Environment*, ed. U. G. Jørgensen (Berlin: Springer), 163

- Tsuji, T. 1981, *J. Astrophys. Astron.*, 2, 95  
———. 1988, *A&A*, 197, 185  
Van der Veen, W. E. C. J., & Rugers, M. 1989, *A&A*, 226, 183  
Wing, R. F., Carpenter, K. G., & Wahlgren, G. M. 1983, *Atlas of High Resolution IUE Spectra of Late-Type Stars*, Perkins Obs. Spec. Publ. No. 1